Journal of the Physical Society of Japan
Vol. 79, No. 6, June, 2010, 064001
©2010 The Physical Society of Japan

Stability Analysis of Attractor Neural Network Model of Inferior Temporal Cortex —Relationship between Attractor Stability and Learning Order—

Tomoyuki KIMOTO*, Tatsuya UEZU[1], and Masato OKADA[2,3]

Oita National College of Technology, Oita 870-0152, Japan
[1]*Graduate School of Sciences and Humanities, Nara Women's University, Nara 630-8506, Japan*
[2]*Graduate School of Frontier Sciences, The University of Tokyo, Kashiwa, Chiba 277-8561, Japan*
[3]*RIKEN Brain Science Institute, Wako, Saitama 351-0198, Japan*

(Received December 7, 2009; accepted March 1, 2010; published May 25, 2010)

Miyashita found that the long-term memory of visual stimuli is stored in the monkey's inferior temporal cortex and that the temporal correlation in terms of the learning order of visual stimuli is converted into spatial correlation in terms of the firing rate patterns of the neuron group. To explain Miyashita's findings, Griniasty *et al.* [Neural Comput. **5** (1993) 1] and Amit *et al.* [J. Neurosci. **14** (1994) 6435] proposed the attractor neural network model, and the *Amit model* has been examined only for the stable state acquired by storing memory patterns in a fixed sequence. In the real world, however, the learning order has statistical continuity but it also has randomness, and the stability of the state changes depending on the statistical properties of learning order when memory patterns are stored randomly. In addition, it is preferable for the stable state to become an appropriate attractor that reflects the relationship between memory patterns by the statistical properties of the learning order. In this study, we examined the dependence of the stable state on the statistical properties of the learning order without modifying the Amit model. The stable state was found to change from the correlated attractor to the Hopfield or M_p attractor, which is the mixed state with all memory patterns when the rate of random learning increases. Furthermore, we found that if the statistical properties of the learning order change, the stable state can change to an appropriate attractor reflecting the relationship between memory patterns.

KEYWORDS: inferior temporal cortex, Miyashita's physiological experiment, Amit model, correlated attractor, learning order, stability
DOI: 10.1143/JPSJ.79.064001

1. Introduction

Miyashita and Chang had a monkey learn 100 fractal patterns and showed that neurons in the monkey's inferior temporal cortex selectively respond to fractal patterns.[1] In a further study, Miyashita had a monkey learn 97 fractal patterns repeated in a fixed sequence and then presented the fractal patterns to the monkey after learning while measuring the firing rate patterns of neurons in the monkey's inferior temporal cortex.[2] He found that the smaller the difference between the learning orders of each presented fractal pattern, the larger the spatial correlation between the corresponding firing rate patterns. Furthermore, he showed that there was mutual spatial correlation among about eight consecutive firing rate patterns in the learning order. Miyashita was thus the first to show that long-term memory of visual stimuli is stored in the monkey's inferior temporal cortex and that the temporal correlation in terms of the learning order of visual stimuli is converted into spatial correlation in terms of the firing rate patterns of a neuron group.

Griniasty *et al.* and Amit *et al.* proposed an attractor neural network model based on the Hopfield model to explain Miyashita's physiological findings.[3,4] They used visual stimuli in the inferior temporal cortex as the memory patterns of their model, and assigned learning order to the memory patterns. Their model stores not only the memory patterns learned by auto-correlation learning but also the adjoining memory patterns learned by cross-correlation learning. Hereafter, we will call their model the *Amit model*. With this modified learning, the memory patterns become unstable even if they are stored. The retrieval process is started by presenting an arbitrary memory pattern to the Amit model after learning, and consecutive memory patterns are mixed into the retrieval state one after another, like a chain reaction. In equilibrium, the retrieval state has the highest spatial correlation with the presented memory pattern, and the correlation graph between the retrieval state and each memory pattern takes the shape of a Gaussian distribution.[3,4] Such a retrieval state in equilibrium is called the *correlated attractor*. When examining the spatial correlation between the correlated attractors that are retrieved from different memory patterns, the smaller the difference between the learning orders of the presented memory patterns, the larger the spatial correlation between the retrieved correlated attractors. Thus, the temporal correlation in terms of the learning order of the memory patterns is converted into spatial correlation in terms of the firing rate patterns of a neuron group, as shown by Miyashita's physiological findings. The Amit model is quite useful because it can be used to explain the physiological findings by assuming only a slight improvement in the learning rule of the Hopfield model. In fact, the basic properties of the Amit model have also been examined by other researchers,[5,6] and the model has been used to explain many of the physiological findings.[7–9] Furthermore, the Amit model has also been applied to transformation-invariant recognition.[10,11)]

*E-mail: kimoto@oita-ct.ac.jp

The Amit model has been examined only when the correlated attractor is acquired by storing the memory patterns in a fixed sequence. In the real world, however, the learning order has statistical continuity, but it also has randomness. Even if the learning rule of the Amit model is fixed, it is predictable that the stability of the state will change depending on the statistical properties of the learning order when memory patterns are stored randomly, and a stable state automatically changes from a correlated attractor to another attractor. We are now investigating the change in the correlated attractor's stability when the statistical properties of the learning order are changed. We also examined whether the memory patterns become stable when the degree of randomness in the statistical property of the learning order becomes larger. Furthermore, we examined whether the stable state can change to an appropriate attractor that reflects the relationship between memory patterns showed by the statistical properties of the learning order.

2. Model

The Amit model is a mutual connection network consisting of N neurons, each of which can take either of two states (± 1). Asynchronous updating at a finite temperature is used.

In asynchronous updating, one neuron is chosen at random from N neurons. For example, let us assume that the ith neuron is chosen. The internal state u_i of the ith neuron is given by

$$u_i = \sum_{j \neq i}^{N} J_{ij} x_j, \tag{1}$$

where J_{ij} is the connection weight from the jth neuron to the ith neuron, and x_j is the jth neuron's state. The probability that state x_i of the ith neuron is ± 1 is determined using u_i:

$$\mathrm{Prob}[x_i = \pm 1] = \frac{1 \pm \tanh(\beta u_i)}{2}, \tag{2}$$

where $\beta = 1/T$ depends on the temperature T.

The memory patterns $\boldsymbol{\xi}^\mu$, $(1 \le \mu \le p)$ stored in the model are N-dimensional vectors consisting of the binary values ± 1. μ is the serial number of a memory pattern, and p is the number of memory patterns. The probability that each element ξ_i^μ of the memory pattern $\boldsymbol{\xi}^\mu$ takes ± 1 is given by

$$\mathrm{Prob}[\xi_i^\mu = \pm 1] = \frac{1}{2}, \quad (1 \le \mu \le p, 1 \le i \le N). \tag{3}$$

In the Amit model, the connection weight J_{ij} from the jth neuron to the ith neuron is determined using

$$J_{ij} = \frac{1}{N} \sum_{\mu=1}^{p} (a\xi_i^\mu \xi_j^{\mu-1} + \xi_i^\mu \xi_j^\mu + a\xi_i^\mu \xi_j^{\mu+1}), \tag{4}$$

where $\xi_i^0 = \xi_i^p$ and $\xi_i^{p+1} = \xi_i^1$. In the learning rule, the memory patterns are stored on the basis of auto correlation learning, and adjoining memory patterns in the learning order are stored on the basis of cross-correlation learning. The correlation learning coefficient between adjoining memory patterns is a. We assume that $J_{ii} = 0$.

In our study, the connection weight J_{ij} is determined using the following rule to take into account the statistical property of the learning order:

$$J_{ij} = \frac{1}{VN} \sum_{v=1}^{V} \sum_{\mu=1}^{p} (a\xi_i^\mu \xi_j^{\nu'} + \xi_i^\mu \xi_j^\mu + a\xi_i^\mu \xi_j^{\nu''}), \quad (\nu' \neq \mu, \nu'' \neq \mu), \tag{5}$$

$$\mathrm{Prob}[(\xi_j^{\nu'} = \xi_j^{\mu-1}) \cap (\xi_j^{\nu''} = \xi_j^{\mu+1})] = b, \tag{6}$$

$$\mathrm{Prob}[(\xi_j^{\nu'} \neq \xi_j^{\mu-1}) \cup (\xi_j^{\nu''} \neq \xi_j^{\mu-1})] = (1 - b), \tag{7}$$

where the repetitive learning of p times in eq. (5) is one learning cycle, and this cycle is repeated V times. In the original Amit model, only one learning cycle needs to store the memory patterns since the learning order is fixed. In the learning rule of eq. (5) used in our study, a very large number of learning cycles are executed because stored memory patterns are stochastically determined. It is assumed that the consecutive learning of the same memory pattern is avoided except the learning corresponding to the second term of eq. (5), that the regular learning proposed by Amit *et al.* is executed with the probability shown in eq. (6), and that the irregular learning is executed with the probability shown in eq. (7). This model corresponds to the original Amit model when $b = 1$. Hereafter, we call the learning rule at $b = 1$ *Amit learning* and the learning rule at $b = 0$ *random learning*. Learning gradually changes from Amit learning to random learning as b changes from one to zero.

We define the overlap between the retrieval state $\boldsymbol{x}$ and the memory pattern $\boldsymbol{\xi}^\mu$ as

$$m_\mu = \frac{1}{N} \sum_{i=1}^{N} \xi_i^\mu \langle x_i \rangle, \tag{8}$$

where $\langle x_i \rangle$ is the thermal mean of x_i. If the thermal mean of retrieval state $\boldsymbol{x}$ is exactly equal to the memory pattern $\boldsymbol{\xi}^\mu$, then m_μ is equal to 1.

3. Theory

To analyze the properties of the retrieval state using statistical mechanics, we transform the synaptic weight J_{ij} of eq. (5) using eqs. (6) and (7) into an analytical form. From the Amit learning and random learning shown in eqs. (6) and (7), when V is very large, the learning rule becomes equivalent to

$$J_{ij} = \frac{1}{N} \sum_{\mu,\nu=1}^{p} \xi_i^\mu A_{\mu\nu} \xi_j^\nu, \tag{9}$$

$$A_{\mu\nu} = \delta_{\mu\nu} + ab(\delta_{\mu,\nu-1} + \delta_{\mu,\nu+1}) + 2\frac{a(1-b)}{p-1}(1 - \delta_{\mu\nu}), \tag{10}$$

where δ is Kronecker's delta. In complete Amit learning, the third term on the right side of eq. (10) is omitted since $b = 1$. In complete random learning, the second term on the right side is omitted since $b = 0$, so auto correlation learning for each memory pattern is executed, and cross-correlation learning with all memory patterns is executed with a probability of $2a/(p-1)$.

To illustrate the property of the retrieval state in equilibrium, we discuss the model in terms of statistical mechanics with regard to the following Hamiltonian H, obtained from eqs. (1), (9), and (10). We consider the case in which the number of neurons N is infinitely large, and the number of memory patterns p is $O(1)$ irrespective of N:

$$H = -\frac{1}{2N}\sum_{i\neq j}^{N}\sum_{\mu,\nu=1}^{p}\xi_i^{\mu}A_{\mu\nu}\xi_j^{\nu}x_i x_j, \tag{11}$$

$$Z = \operatorname*{Tr}_{\boldsymbol{x}}\exp(-\beta H), \tag{12}$$

$$f = -\frac{1}{\beta N}\log Z, \tag{13}$$

where Z is the partition function and f is the free energy. Using the saddle-point method, we obtain the free energy

$$f = \frac{1}{2}\sum_{\mu,\nu=1}^{p} m_\mu A_{\mu\nu} m_\nu - \frac{1}{\beta}\left\langle\!\!\left\langle \log\left[2\cosh\left(\beta\sum_{\mu,\nu=1}^{p} m_\mu A_{\mu\nu}\xi_i^{\nu}\right)\right]\right\rangle\!\!\right\rangle, \tag{14}$$

where $\langle\langle\phi\rangle\rangle$ stands for the average over the memory patterns $\boldsymbol{\xi} = (\xi^1,\ldots,\xi^p)$, that is $\langle\langle\phi\rangle\rangle = (1/2^p)\sum_{\{\xi^\mu=\pm1\}}\phi$. Using $\partial f/\partial m_\mu = 0$, we obtain the order parameter equation that determines m_μ that minimizes the free energy:

$$m_\mu = \langle\langle \xi_i^\mu \tanh(\beta u_i)\rangle\rangle, \tag{15}$$

$$u_i = \sum_{\mu,\nu=1}^{p}\xi_i^\mu A_{\mu\nu} m_\nu. \tag{16}$$

The physical meaning of m_μ is the overlap shown in eq. (8).

The evolution equation for the overlap m_μ is obtained as follows in accordance with the study by Uezu *et al.*[8]

$$\frac{\mathrm{d}m_\mu}{\mathrm{d}t} = -m_\mu + \langle\langle \xi_i^\mu \tanh(\beta u_i)\rangle\rangle, \tag{17}$$

$$u_i = \sum_{\mu,\nu=1}^{p}\xi_i^\mu A_{\mu\nu} m_\nu. \tag{18}$$

Using this evolution equation of the order parameter, we can examine the retrieval process of the model. The stationary state of eq. (17) agrees with eq. (15), which describes the retrieval state in equilibrium.

4. Results

As described above, in the Amit model, consecutive memory patterns are mixed into the retrieval state one after another, like a chain reaction, because it stores consecutive memory patterns by cross-correlation learning, as shown in eq. (4). The parameters a, b, and T determine how many memory patterns are mixed into the retrieval state in equilibrium. Figure 1 shows three typical attractors that can become stable states in the Amit model. The horizontal axis shows the serial number of the memory pattern μ, and the vertical axis shows the overlap between memory patterns and the retrieval state. Figure 1(a) shows a correlated attractor. The correlated attractor in the figure is retrieved by presenting the 7th memory pattern. The correlation function has a shape like a Gaussian distribution function with consecutive memory patterns. The chain reaction of the retrieval process stops when about four consecutive memory patterns are mixed into the retrieval state. The width of this chain reaction changes depending on the parameters a, b, and T. We will call the attractor shown in Fig. 1(b) the *Hopfield attractor*. The Hopfield attractor in the figure is retrieved by presenting the 7th memory pattern. The chain reaction does not occur greatly, so the Hopfield attractor is the retrieval state that has a large spatial correlation with the presented memory pattern, a small spatial correlation with the adjoining memory patterns, and a zero spatial correlation with other memory patterns. As shown in the figure, it is almost the same as the presented memory pattern since $m_7 \sim 1.0$; however, we do not call it the memory pattern,

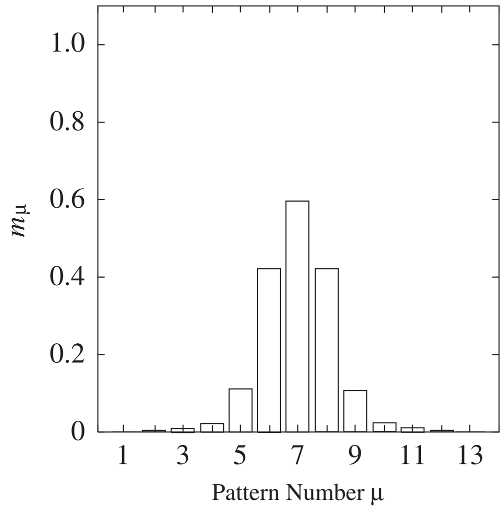

(a)

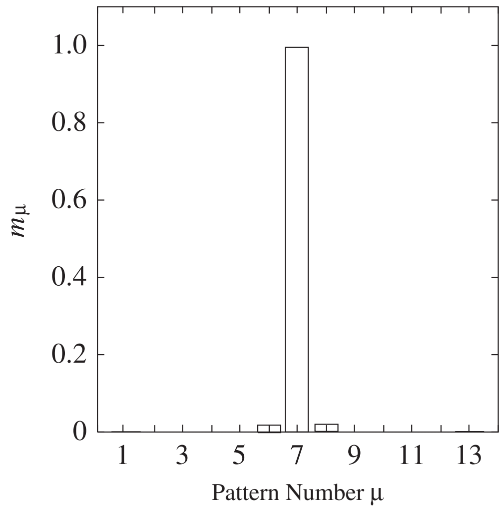

(b)

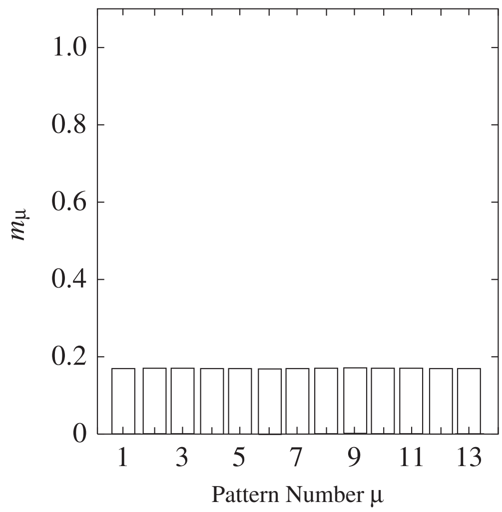

(c)

Fig. 1. Three types of attractors in Amit model: (a) correlated attractor, (b) Hopfield attractor, and (c) M_p attractor.

instead the Hopfield attractor because the adjoining memory patterns are included a bit in the retrieval state. We call the attractor shown in Fig. 1(c) the *M_p attractor*. It is the retrieval state in which the chain reaction extends to all memory patterns. All overlaps m_1–m_p have the same value because the M_p attractor is the retrieval state into which all memory patterns are mixed with symmetry.

Figure 2 shows the phase diagram of these three attractors at $p = 21$. To obtain Fig. 2, we used the method described below. Each attractor was presented as the initial state of the model, and the retrieval dynamics shown in eqs. (1) and (2) was repeated until the network reaches the equilibrium state. We then examined whether the attractor maintains its stability for various a, b, and T values. First, we explain the phase diagram of the original Amit model shown in Fig. 2(a) with $b = 1.0$. The broken line is the critical temperature T_c below which the correlated attractor remains stable. It increases rapidly at approximately $a = 0.35$ and subsequently decreases gradually as a increases to 1.0. The solid line is the critical temperature T_c below which the Hopfield attractor remains stable. It decreases as a increases, and the Hopfield attractor becomes unstable at $a > 0.5$. The dotted line is the critical temperature T_c of the M_p attractor. The inside of the oval arc extending to approximately $a = 0.7$ is an unstable area of the M_p attractor. At $a < 0.7$, the M_p attractor is stable at low temperatures, and becomes unstable if temperature is increased; then it becomes stable again if temperature is further increased. In previous studies, the temporary unstable area for the M_p attractor surrounded by the oval arc shown in Fig. 2(a) has not been found. At $0 < a < 1$, the dotted line rising sharply toward the upper right continues to increase linearly outside the frame and reaches $T_c = 3.0$ at $a = 1.0$. As mentioned above, the Amit model has multiple stability, and the number of stable states depends on the values of the parameters such as a and T.

The closed/open circles are used in explaining of Fig. 3. Next, the results obtained when the rate of random learning was increased by decreasing b, are shown in Figs. 2(b) and 2(c). For the correlated attractor, the stable area shown in Fig. 2(b) becomes smaller than that shown in Fig. 2(a); it disappears in Fig. 2(c). For the Hopfield attractor, the stable area shown in Figs. 2(b) and 2(c) gradually extends toward the right as b is decreased. For the M_p attractor, the temporary unstable area disappears in Figs. 2(b) and 2(c). On the other hand, there is no change in the dotted line rising sharply toward the upper right.

Figure 3 shows the phase diagram that represents the horizontal axis as b. The horizontal axis on the far right ($b = 1.0$) corresponds to complete Amit learning, and the horizontal axis on the far left ($b = 0$) corresponds to complete random learning. The closed/open circles at $b = 1.0$ shown in Fig. 3 correspond to those shown in Fig. 2(a). The lines correspond to the theoretical values, and the error bars show the average value and standard deviation from computer simulation. To obtain Fig. 3, we used a method similar to that described above: Each attractor was presented as the initial state of the model, and we examined whether the attractor maintains its stability for various a, b, and T values. In the simulation, we examined T_c at $N = 20{,}000$ or greater. The simulation results correspond well to the lines for the theoretical values.

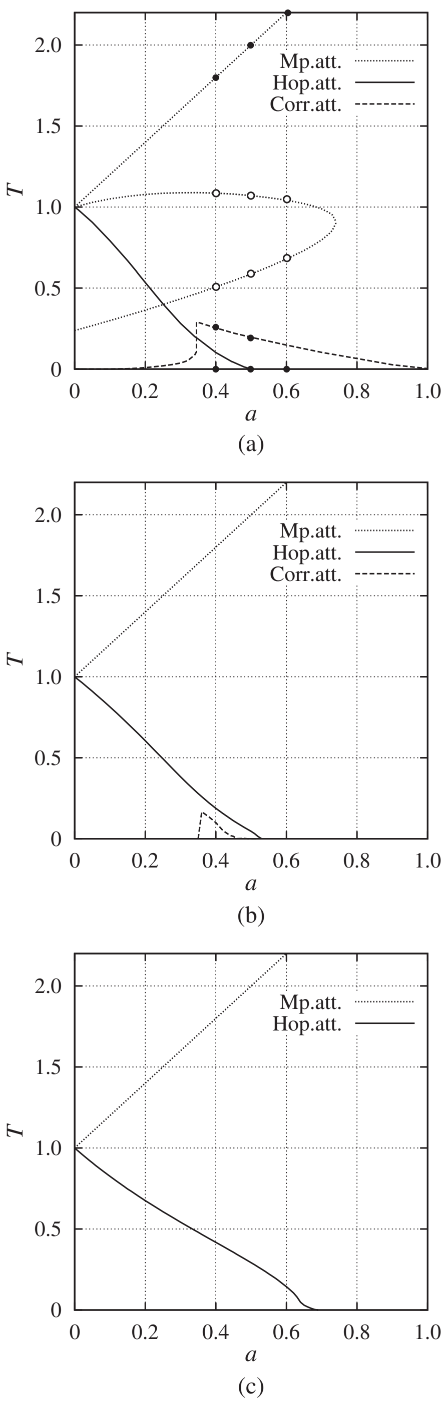

Fig. 2. Phase diagram representing horizontal axis as a ($p = 21$): (a) $b = 1.0$, (b) $b = 0.8$, and (c) $b = 0.3$. (a) Phase diagram for the original Amit model. The broken line is the critical temperature T_c below which the correlated attractor remains stable, and the solid line is the critical temperature T_c below which the Hopfield attractor remains stable. The dotted line extending toward the upper right is the critical temperature T_c below which the M_p attractor remains stable, but the inside of the oval arc is an unstable area of the M_p attractor. (b,c) Phase diagrams obtained when the rate of random learning was increased.

For the correlated attractor with $a = 0.4$, as b decreases from 1.0, the T_c of the attractor also decreases, and the attractor becomes unstable at $b = 0.73$. For the Hopfield attractor, as b decreases from 1.0, T_c increases. The T_c of the M_p attractor does not depend on b and is constant at $T_c = 1.8$. In addition, the temporary unstable area between the two open circles for the M_p attractor at $b = 1$ disappears

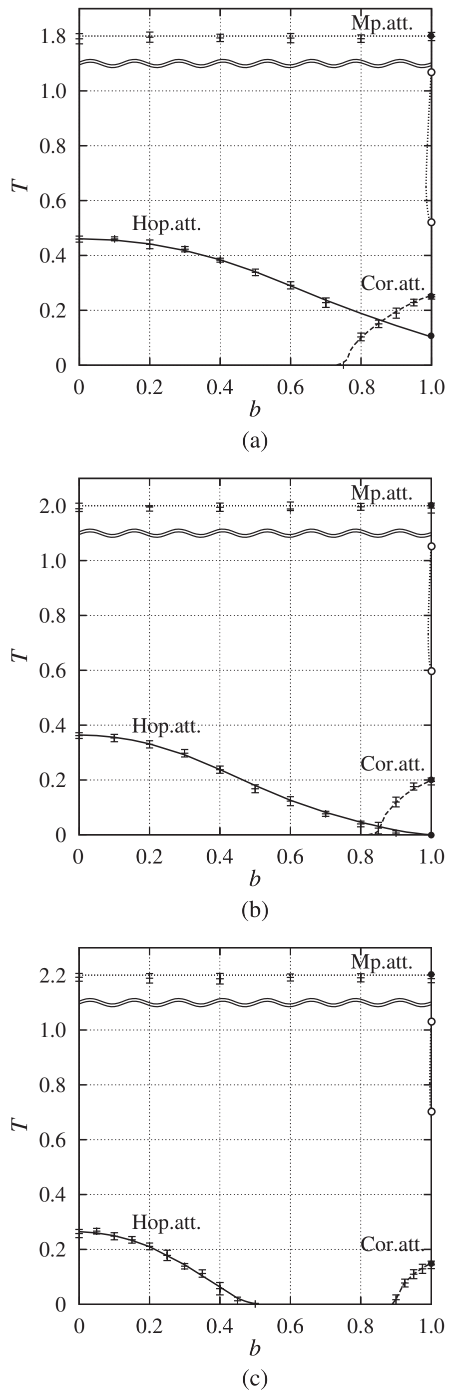

Fig. 3. Phase diagram representing horizontal axis as b ($p = 21$): (a) $a = 0.4$, (b) $a = 0.5$, and (c) $a = 0.6$. Three kinds of lines show the critical temperature T_c below which the correlated, Hopfield, and M_p attractors remain stable. However, the M_p attractor is unstable in the narrow area enclosed by the broken line and open circles on the far right of the diagram.

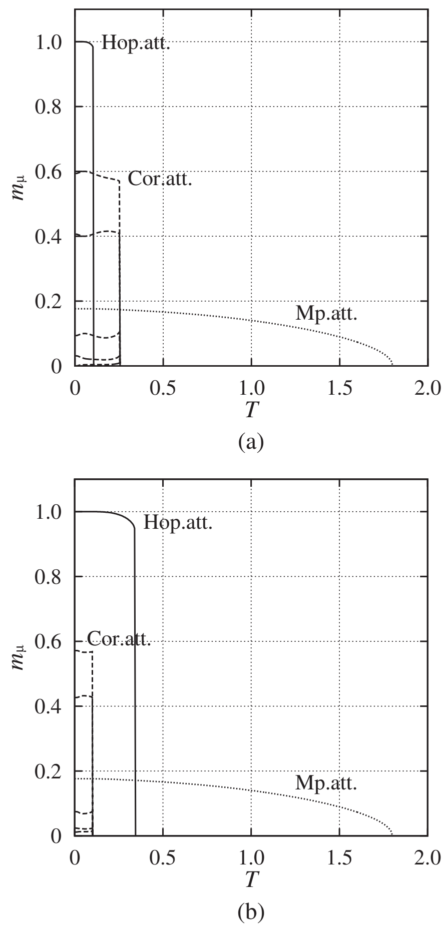

Fig. 4. Overlap m_μ values for various temperatures T ($p = 21$, $a = 0.4$): (a) Amit Learning (for $b = 1.0$) and (b) Amit+Random Learning (Hopfield attractor and M_p attractor for $b = 0.5$, correlated attractor for $b = 0.8$).

rapidly when b decreases from 1.0. Similarly, for $a = 0.5$, as b decreases from 1.0, The T_c of the correlated attractor decreases, and the attractor becomes unstable at $b = 0.85$. Although the Hopfield attractor was unstable at $b = 1.0$, when b decreases from 1.0, T_c increases. The M_p attractor shows the same property as the M_p attractor with $a = 0.4$. Similarly, for $a = 0.6$, when b decreases from 1.0, the T_c of the correlated attractor decreases, and the attractor becomes unstable at $b = 0.9$. The Hopfield attractor becomes stable at $b < 0.5$. When b decreases from 0.5, the T_c of the Hopfield attractor increases. For $0.5 < b < 0.9$, the Hopfield and correlated attractors are unstable; only the M_p attractor remains stable. The M_p attractor shows the same property as the M_p attractor with $a = 0.4$ and 0.5. The random learning reduces the T_c of the correlated attractor and increases that of the Hopfield attractor.

Figure 4 shows the aspect of the phase transition of the overlap m_μ. Each attractor overlaps with memory patterns, as shown in Fig. 1. Therefore, the retrieval state for the correlated attractor is shown by the many lines of $m_\mu \sim 0.6$, 0.4, 0.1, and 0.05, the retrieval state for the Hopfield attractor is shown by the line of $m_\mu \sim 1.0$, and the retrieval state for the M_p attractor is shown by the line of $m_\mu \sim 0.18$. The phase transition temperatures in Fig. 4(a) correspond to those at $b = 1.0$ shown in Fig. 3(a), and the phase transition temperatures in Fig. 4(b) correspond to those at $b < 1.0$ shown in Fig. 3(a). Figure 4 shows that, regardless of b, the first-order phase transition occurs for the Hopfield and correlated attractors, and the second-order phase transition occurs for the M_p attractor. Although the results for the other parameters are omitted here, the orders of the phase transitions for the three attractors for various values of a and b are the same as those for $a = 0.4$ and $b = 1$.

The phase diagram in Fig. 3 shows the attractor's stability when the attractor is presented as the initial state, and the retrieval dynamics shown in eqs. (1) and (2) is repeated at a temperature lower than T_c. Thus, a few attractors can become bistable states when each attractor is presented as the initial state. For example, in Fig. 3(c), both the correlated and M_p attractors become bistable states at $a = 0.6$, $b = 0.95$, and $T = 0.1$, and both the Hopfield and M_p attractors become bistable states at $a = 0.6$, $b = 0.3$, and $T = 0.1$. However, it is important to identify which attractor is retrieved from the memory pattern because the memory pattern is presented as the initial state in an actual situation. It is easy to predict which attractor is retrieved from the memory pattern using Fig. 3. The retrieval state changes one after another as "the presented memory pattern → the Hopfield attractor → the correlated attractor → M_p attractor" by the chain reaction mechanism of the learning rule, and the transition of the retrieval state stops at the stable attractor that was retrieved earlier during the retrieval process. For example, although both the correlated and M_p attractors become bistable states at $a = 0.6$, $b = 0.95$, and $T = 0.1$ in Fig. 3(c), it is predicted that the retrieval state will become the correlated attractor in equilibrium because it is retrieved earlier than the M_p attractor. Similarly, although both the Hopfield and M_p attractors become bistable states at $a = 0.6$, $b = 0.3$, and $T = 0.1$ in Fig. 3(c), it is predictable that the retrieval state becomes the Hopfield attractor in equilibrium because it is retrieved earlier than the M_p attractor. Moreover, since only the M_p attractor becomes the stable state at $a = 0.6$, $b = 0.7$, and $T = 0.1$ in Fig. 3(c), it is predictable that the retrieval state becomes the M_p attractor in equilibrium. Figure 5 shows the results of numerical calculation using the overlap dynamics shown in eq. (17) for the three parameters mentioned above, when the memory pattern is presented as the initial state. In accordance with the prediction, the trajectory shown in Fig. 5(a) points toward the state that corresponds to the correlated attractor shown in Fig. 1(a), the trajectory shown in Fig. 5(b) points toward the state that corresponds to the Hopfield attractor shown in Fig. 1(b), and the trajectory shown in Fig. 5(c) points toward the state that corresponds to the M_p attractor shown in Fig. 1(c). Although the results for the other parameters are omitted, it was numerically confirmed that trajectories converged to the predicted states for various values of a, b, and T.

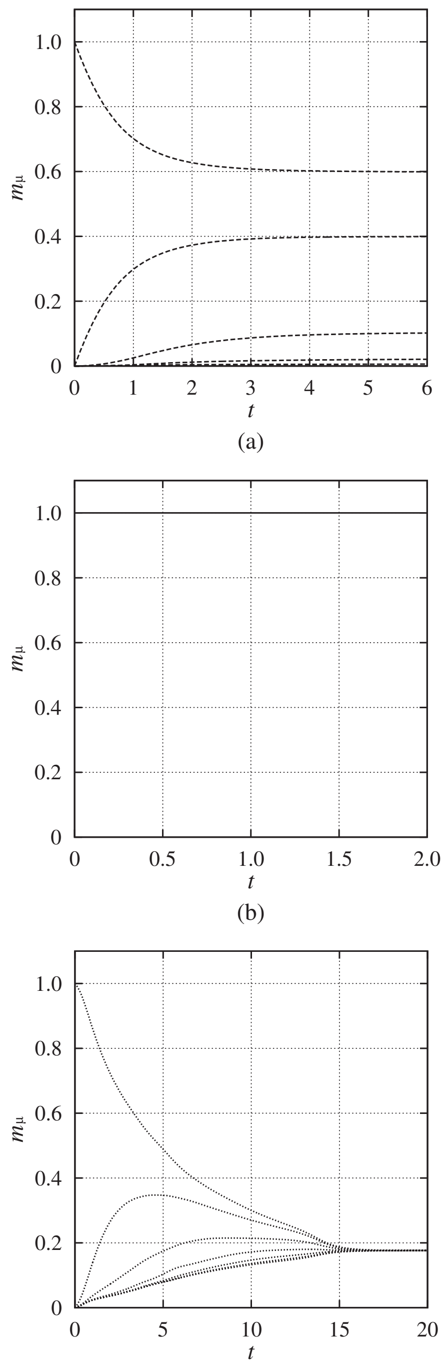

Fig. 5. Overlap m_μ for retrieval time t ($p = 21$, $a = 0.6$, and $T = 0.1$): (a) correlated attractor ($b = 0.95$), (b) Hopfield attractor ($b = 0.3$), and (c) M_p attractor ($b = 0.7$).

5. Conclusion

Miyashita showed that the temporal correlation in terms of the learning order of visual stimuli is converted into spatial correlation in terms of the firing rate patterns of a neuron group, in the monkey's inferior temporal cortex. To explain Miyashita's findings, Griniasty *et al.* and Amit *et al.* proposed the attractor neural network model demonstrating that the memory patterns are converted to the correlated attractor.

The Amit model has been examined only when the correlated attractor is acquired by storing the memory patterns in a fixed sequence. In the real world, however, the learning order has statistical continuousness, but it also has randomness. The stability of the correlated attractors should change in accordance with the statistical properties of the learning order. Therefore, we examined the stability of the attractor on the Amit model when the degree of randomness becomes large. We found that the stability of the correlated attractor has weakened gradually when the rate of the random learning increased. Furthermore, we examined what type of attractor becomes a stable state in accordance with the statistical properties of the learning order. We found that the stable state changed from the correlated attractor to the M_p attractor when the rate of the random learning increased, and the stable state changed from the M_p attractor to the Hopfield attractor when the rate of the random learning further increased.

It is preferable for the stable state to become an appropriate attractor that reflects the statistical properties of the learning order because the learning order has information on the relationship between memory patterns. Here, we consider whether the correlated, M_p, and Hopfield attractors appropriately reflect the relationship between memory patterns. If the learning order is always fixed, not only information that consecutive memory patterns have the mutual relation but also information on the learning order is important. In this case, the stable state of the model becomes the correlated attractor that reflects the relationship between the memory patterns, and the learning order. If the randomness of the learning order is strong, the possibility that the memory patterns are unrelated and independent mutually is high. In this case, the stable state of the model becomes the Hopfield attractor that shows only one memory pattern. If the learning order has moderate continuity, the possibility that the memory patterns have mutual relation but have no information on the learning order is high. In this case, the stable state of the model becomes the M_p attractor, which indicates that the memory patterns have mutual relation but have no information on the learning order. As mentioned above, we think that when the statistical properties of the learning order change, the stable state can change to an the appropriate attractor reflecting the relationships between memory patterns.

Acknowledgements

This work was partially supported by a Grant-in-Aid for Scientific Research on Priority Areas No. 18079003, Grants-in-Aid for Scientific Research (A) No. 20240020 and (C) No. 22500216 from the Ministry of Education, Culture, Sports, Science and Technology of Japan.

1) Y. Miyashita and H. S. Chang: Nature **331** (1988) 68.
2) Y. Miyashita: Nature **335** (1988) 817.
3) M. Griniasty, M. V. Tsodyks, and D. J. Amit: Neural Comput. **5** (1993) 1.
4) D. J. Amit, N. Brunel, and M. V. Tsodyks: J. Neurosci. **14** (1994) 6435.
5) T. Fukai, T. Kimoto, M. Doi, and M. Okada: J. Phys. A **32** (1999) 5551.
6) S. Tanimoto, M. Okada, T. Kimoto, and T. Uezu: J. Phys. Soc. Jpn. **75** (2006) 104004.
7) A. Samsonovich and B. L. McNaughton: J. Neurosci. **17** (1997) 5900.
8) T. Uezu, A. Hirano, and M. Okada: J. Phys. Soc. Jpn. **73** (2004) 867.
9) T. Kimoto, T. Uezu, and M. Okada: J. Phys. Soc. Jpn. **77** (2008) 124002.
10) M. S. Bartlett and T. J. Sejnowski: Comput. Neural Syst. **9** (1998) 399.
11) N. Parga and E. Rolls: Neural Comput. **10** (1998) 1507.